

# Intercombination transition rates in Al-like Au<sup>66+</sup> ions

E. Träbert<sup>1,a</sup>, U. Staude<sup>2</sup>, P. Bosselmann<sup>2</sup>, K.H. Schartner<sup>2</sup>, P.H. Mokler<sup>3</sup>, and X. Tordoir<sup>4</sup>

<sup>1</sup> Experimentalphysik III, Ruhr-Universität Bochum, 44780 Bochum, Germany

<sup>2</sup> I. Physikalisches Institut, Universität Giessen, 35392 Giessen, Germany

<sup>3</sup> Gesellschaft für Schwerionenforschung, 64291 Darmstadt, Germany

<sup>4</sup> Physique Nucléaire Expérimentale, Université de Liège, 4000 Liège, Belgium

Received: 23 February 1998 / Accepted: 5 March 1998

**Abstract.**  $N = 3$ ,  $\Delta n = 0$  intercombination transitions in Al-like ions of Au have been studied by time-resolved EUV spectroscopy of foil-excited ion beams. Wavelengths and lifetimes are compared to the available relativistic calculations. The theoretical data are found to be useful for guidance, but of clearly insufficient precision, in particular for the transition probabilities.

**PACS.** 32.30.Jc Visible and ultraviolet spectra – 32.70.Fw Absolute and relative intensities – 34.50.Fa Electronic excitation and ionization of atoms (including beam-foil excitation and ionization)

## 1 Introduction

From low to high nuclear charge  $Z$ , some atomic systems develop in peculiar ways along isoelectronic sequences. For most heavy, highly charged ions not even the lowest excited levels have ever been measured. Part of the experimental problem lies in the fact that the excitation energies of different levels scale with  $Z$ ,  $Z^2$ , or  $Z^4$ . These scalings move the observable transitions from the visible range of the spectrum to the extreme uv (EUV) or the x-ray range. The increasing fine structure intervals can also cause changes in the sequence of levels. For example, in the Al isoelectronic sequence, Zilitis [1] notes 11 such pairwise changes among the lowest 10 levels. Similarly, the scaling of the electric dipole (E1) transition probabilities with  $Z$  or  $Z^4$  renders most level lifetimes in highly charged ions too short for any conventional measurement. A systematic exception to this are the transitions which at low  $Z$  ( $LS$ -coupling notation) are termed intercombination transitions. Even at high  $Z$ , near the  $jj$ -coupling limit, their probabilities remain lower than those of the corresponding resonance transitions by several orders of magnitude. We aimed at observations of such transitions including the measurement of transition probabilities.

For this investigation we chose highly charged Au ions in order to complement our previous studies on Xe ( $Z = 54$ ) and Au ( $Z = 79$ ) [2, 3 (henceforth called Paper I)]. In those earlier investigations the emphasis was on measurements of the resonance transitions  $3s-3p$  of the Na-like ions. The same spectra, however, contained  $3s-3p$  intercombination transitions in Mg- and (weakly) Al-like ions of the same elements, and we wanted to improve our observations of those. Although these systems with their

two or three electrons in an open shell, respectively, are more complex than the Na-like system and may thus seem to be of less fundamental interest, we see additional features which deserve scrutiny and testing their theoretical description. One such problem is why the addition of just one more electron (Mg sequence) poses such problems for precise calculations even at low  $Z$  (see discussions in [4, 5]). Moreover, a notable deviation of measured intercombination transition probabilities from predicted ones has been observed, in a range of fairly high nuclear charges [6, 7].

Another point of interest is the detailed isoelectronic trend of the level structure and transition probabilities in the  $3s^2 3p^2 P^o - 3s 3p^2 ^4 P$  multiplet in the Al I isoelectronic sequence: At low  $Z$ , the fine structure intervals of the ground and excited terms are small compared to the mean transition energy, resulting in a line multiplet which appears with a characteristic intensity pattern in various laboratory light sources and in the light of the solar corona [9, 10]. In particular, the  $J = 3/2 - J' = 5/2$  transition (an unbranched decay of the level that is favoured in population by the highest statistical weight factor  $(2J + 1)$ ) stands out, accompanied on the short-wavelength side by the much weaker  $J = 1/2 - J' = 1/2$  transition.

Relativity, however, changes the compositions of the levels as well as the relative amount of fine structure and electrostatic energy intervals (see Fig. 1 for an illustration of the level scheme). Consequently the lines of the multiplet move apart on the wavelength scale, and the relative line intensities change. In particular, the weak  $J = 1/2 - J' = 3/2$  component, which (for low nuclear charges) is on the short-wavelength end of the line multiplet, gains from the  $\nu^3$  frequency dependence of the transition probability and becomes the stronger decay branch

<sup>a</sup> e-mail: traebert@EP3.ruhr-uni-bochum.de

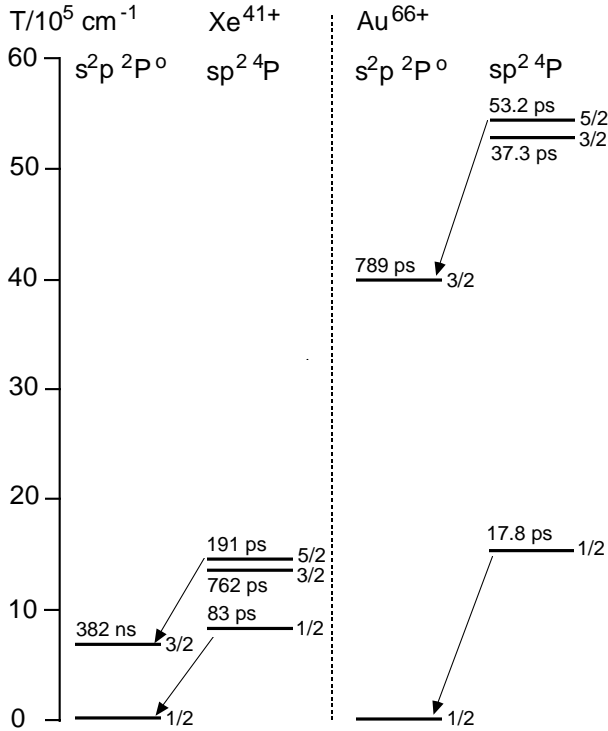


**Fig. 1.** Calculated levels and lifetimes [11] for the lowest 5 levels of Al-like ions of Xe ( $Z = 54$ , left) and Au ( $Z = 79$ , right). The transitions of principal interest,  $3s^23p^2P_{1/2}^o - 3s3p^2^4P_{1/2}$  and  $3s^23p^2P_{3/2}^o - 3s3p^2^4P_{5/2}$ , are indicated.

of the  $J' = 3/2$  level at high  $Z$ . Near  $Z = 79$  (Au), this short-wavelength branch outweighs the other by about a factor of ten in transition probability [11]. Because of the quantum mechanical peculiarity of a matrix element, the upper level of this line,  $^4P_{3/2}$ , is much longer lived than the other two levels of the same term at low  $Z$  [11, 12]. At high  $Z$ , however, the  $^4P_{5/2}$  level is the longest lived [11]. One multiplet component, the  $J = 3/2 - J' = 1/2$  line, even vanishes when the level sequence changes, that is when the ground state fine structure interval grows larger than the  $3s-3p$  energy difference (near  $Z = 58$  [11]). Then the upper level ( $J = 3/2$ ) of the  $3s^23p^2P^o$  ground term crosses the position of the  $J' = 1/2$  level of the excited (displaced) term  $3s3p^2^4P$ , and thereafter it lies higher in excitation energy. As a consequence of this, the lifetime pattern in the multiplet varies substantially. Also, it has been found that the difference of experimental [9, 10, 13, 14] and calculated wavelength data [11] seemed to follow a smooth trend as in many isoelectronic sequences, but only with data for  $Z \leq 42$  [15]. New data near  $Z = 40$  [16] claim a change of the trend and cast doubt on the tentative line identifications for Xe and Au in Paper I, which were based on the validity of the theoretical trend [11]. Similar problems have been noted for the Si isoelectronic sequence [16], in a comparison with again Multi-Configuration Dirac-Fock (MCDF) calculations by Huang [17]. It would be interesting to follow these changes in detail in order to verify the one or other interpretation and

to study the details of the available relativistic calculations as a function of  $Z$ . However, that would be beyond the scope of this study, in which we concentrate on a single high- $Z$  example to be contrasted with some earlier results obtained at lower  $Z$ .

## 2 Experiment

The experiment was done at the UNILAC accelerator of the Gesellschaft für Schwerionenforschung (GSI) at Darmstadt, by basically standard beam-foil techniques [2, 3, 18, 19]. For  $^{197}\text{Au}$  ions at an energy of 12.7 MeV/amu were available, the present maximum energy at the UNILAC accelerator. However, this energy is somewhat lower than optimum for the production of (Mg-like)  $\text{Au}^{67+}$  ions [20, 21]. In fact, the equilibrium charge state distribution measured after passage through a  $500 \mu\text{g}/\text{cm}^2$  thick foil, which reduces the ion energy to about 12.4 MeV/amu, was found to be centered near charge state  $q = 65+$  (Si-like ions). The beam was used in either of two modes (compare Paper I): For survey spectra, the full ion beam of up to 100 nA particles was sent to a standard beam-foil chamber and stripped and excited there by being passed through a  $400 \mu\text{g}/\text{cm}^2$  carbon foil. Alternatively, in order to obtain spectra with a lower background, the ion beam was pre-stripped in the aforementioned  $500 \mu\text{g}/\text{cm}^2$  foil, and a charge-state selected beam ( $q = 66+$ ,  $67+$ ) of up to 8 nA particles was sent to the experiment where it would be passed through a thin ( $50$  or  $90 \mu\text{g}/\text{cm}^2$ ) foil where the charge state might change by up to two units (predominantly towards equilibrium, near  $q = 65+$ ). The carbon foils were mounted on frames with an opening of 10 mm diameter. The geometry of the ion beam was controlled by grids before and behind the experimental chamber. Finally, the ions were dumped in a deep, shielded and biased Faraday cup for signal normalization.

The EUV light emitted after foil-excitation was observed by means of a 5 m grazing-incidence spectrometer [22] equipped with a 270 l/mm grating and a position-sensitive detector. The latter consists of a 40 mm wide microchannelplate (MCP) and a wedge-and-strip anode for two-dimensional read-out. At each position, the detector covered a wavelength interval of about 3 nm. The foil could be displaced by up to 10 cm to permit the recording of decay curves and of delayed spectra. Of this only 7 mm were used, corresponding to a multiple of the decay length of the longest-lived level studied here. Details of the set-up and of the data collection and evaluation procedures for spectra have been published in earlier papers ([2, 19, 22] and Refs. therein).

The optical axis of the spectrometer was adjusted to  $90^\circ$  with respect to the ion beam trajectory. VUV light from a Penning discharge lamp, providing Ne- and Al-ion lines, was used to optimize the detector setting with respect to the Rowland circle, and to measure the dispersion. This latter radiation emanates from a stationary emitter, whereas the spectra of interest are emitted from ions moving at a considerable fraction of the speed of light; hence the first and second order Doppler shifts need to be taken

into account ( $\beta = v/c = 0.1616$ ). At the level of precision needed for this experiment, this is possible from the known ion velocity and the precisely set observation angle. An additional coarse reference point is supplied by the  $K_\alpha$  radiation from the carbon foil, which in third diffraction order came close to the second diffraction order images of the lines of present interest. This also served to establish the position of the foil with respect to the line of sight of the spectrometer. The foil displacement was monitored with  $5\ \mu\text{m}$  precision by a moiré fringe length gauge.

The spectrometer slit width was mostly set to  $100\ \mu\text{m}$ , resulting in an observed line width (FWHM) of  $0.085\ \text{nm}$ . This is a superposition of the value ( $0.074\ \text{nm}$ ) expected (for a stationary light source) from geometry, Doppler broadening because of the finite angle of acceptance of the spectrometer ( $0.007$  to  $0.01\ \text{nm}$ ), and the spatial resolution of the position-sensitive detector which may be as good as  $100\ \mu\text{m}$ . This total line width value is only about 15% more than the value expected from geometry alone and represents a clear improvement compared to Paper I, in addition to the better spectral resolution available now by working in second diffraction order of a grating of almost similar groove density.

In order to reduce the ion beam related background in the spectra, the signal was electronically gated to match the pulse structure of the ion beam. One pulse structure results from the 3 ms pulses of the ion extraction from the Penning type ion source with repetition frequencies ranging from 10 to 50 Hz, the other from the 27 MHz radiofrequency of the linear accelerator system. By such time gating, photons and  $\gamma$  rays produced by ions at some apertures sufficiently far away from the interaction zone would be suppressed because of the travel time of the ion beam, as well as neutrons from nuclear reactions because of their travel time from production to the detector. However, a considerable part of the signal background was found to result from particles (secondary electrons and ions) striking the slit jaw of the spectrometer when it was more than about a millimeter behind the exciter foil. This background contribution showed a time distribution which varied notably as a function of the foil position. Data were recorded in list mode, with those events which passed the hard-wired coincidence conditions of the three electrodes of the position-sensitive detector being stored along with the time information relative to the accelerator pulse structure. In this way, various time window settings could be tested even after the recording of the data, and very clean spectra be obtained by suitable projections.

### 3 Data

With the exciter foil positioned just outside of the field of view of the spectrometer (for maximum light intensity while avoiding the background light from the irradiated foil), the wavelength range of interest ( $6.4$  to  $7.9\ \text{nm}$ ) was observed in second diffraction order, and parts of it also in third and fourth diffraction order. In this range we expected to see one of the resonance lines of the Na-like ion,  $3s-3p_{1/2}$ , the  $3s^2\ ^1S_0-3s3p\ ^3P_1^o$  intercombination transition in the Mg-like ion, two of the

$3s^23p\ ^2P^o-3s3p^2\ ^4P$  transitions in the Al-like ion and the two  $3s^23p^2\ ^3P_{1,2}-3s3p^3\ ^5S_2^o$  transitions in the Si-like ion. Theoretical estimates of transition wavelengths and level lifetimes in Mg-, Al- and Si-like ions are available [8, 11, 12, 17], mostly from MCDF calculations. In the absence of systematic data over wide parts of the isoelectronic sequences, such estimates are needed to guide the experiment and the line identification. As the ion beam energy was lower than before, and since excitation by electron capture has often been found to be more efficient than direct excitation in high-energy ion-foil interaction [23], the spectra were expected to show lines of Al- and Si-like ions more intensely than those of the Mg- and Na-like ions. The latter two, in fact, did not show at all in our new spectra.

The more prominent lines were seen in separate third and fourth order spectra as well. For all these spectra of the foil-excited ion beam, wavelength comparison spectra were obtained from a Penning discharge. We also observed a number of very weak lines which show up only in considerably delayed spectra and appear to represent lifetimes much longer than the about 50 ps of our most prominent line. The identity of these lines - their charge state of origin, multipole order or classification - is not clear. Some of them may be forbidden (M1/E2) fine structure transitions, for which predictions are notoriously imprecise. Unfortunately these lines are too weak to permit useful lifetime measurements.

Spectra typically required half an hour to one hour of observation time each, at the better ion currents. They were analyzed by fitting Gaussian line profiles to the data. In most spectra the lines of interest showed a signal (integrated over the line profile) of a few hundred to more than 1000 counts. This went along with a line width (FWHM) of order 20 channels. The background summed over the full line was typically of the same order of magnitude as the signal after background subtraction. The statistical uncertainty is then strongly affected by that of the background, which was lower and under better control than in Paper I.

Our ion beam spectra cover continuously the wavelength range 11 to 17 nm (Fig. 2). They contain only a single fairly intense line, at a wavelength of  $7.27 \pm 0.01\ \text{nm}$  (assuming observation in second diffraction order). The same line has been seen in third and fourth diffraction order spectra. From the charge-state distribution of the ions after foil passage, its wavelength and decay properties, as well as from experience with spectra for lower- $Z$  members of the isoelectronic sequence, we assign it to the transition  $3s^2\ 3p\ ^2P_{3/2}^o-3s\ 3p^2\ ^4P_{5/2}$  in the Al-like ion Au<sup>66+</sup>. Nearby weaker lines are numerous, but - except for one other transition in the same multiplet - too weak to be positively assigned to any particular ionization stage (Tab. 1). Although a weak line appears at the calculated wavelength  $6.997\ \text{nm}$  [24] of the  $3s\ ^2S_{1/2}-3p\ ^2P_{1/2}^o$  transition in Na-like Au<sup>68+</sup>, it has to be suspected of a different origin, as the ion beam energy is too low for a notable Na-like charge state fraction under our conditions. The  $3s^2\ ^1S_0-3s\ 3p\ ^3P_1^o$  intercombination transition in

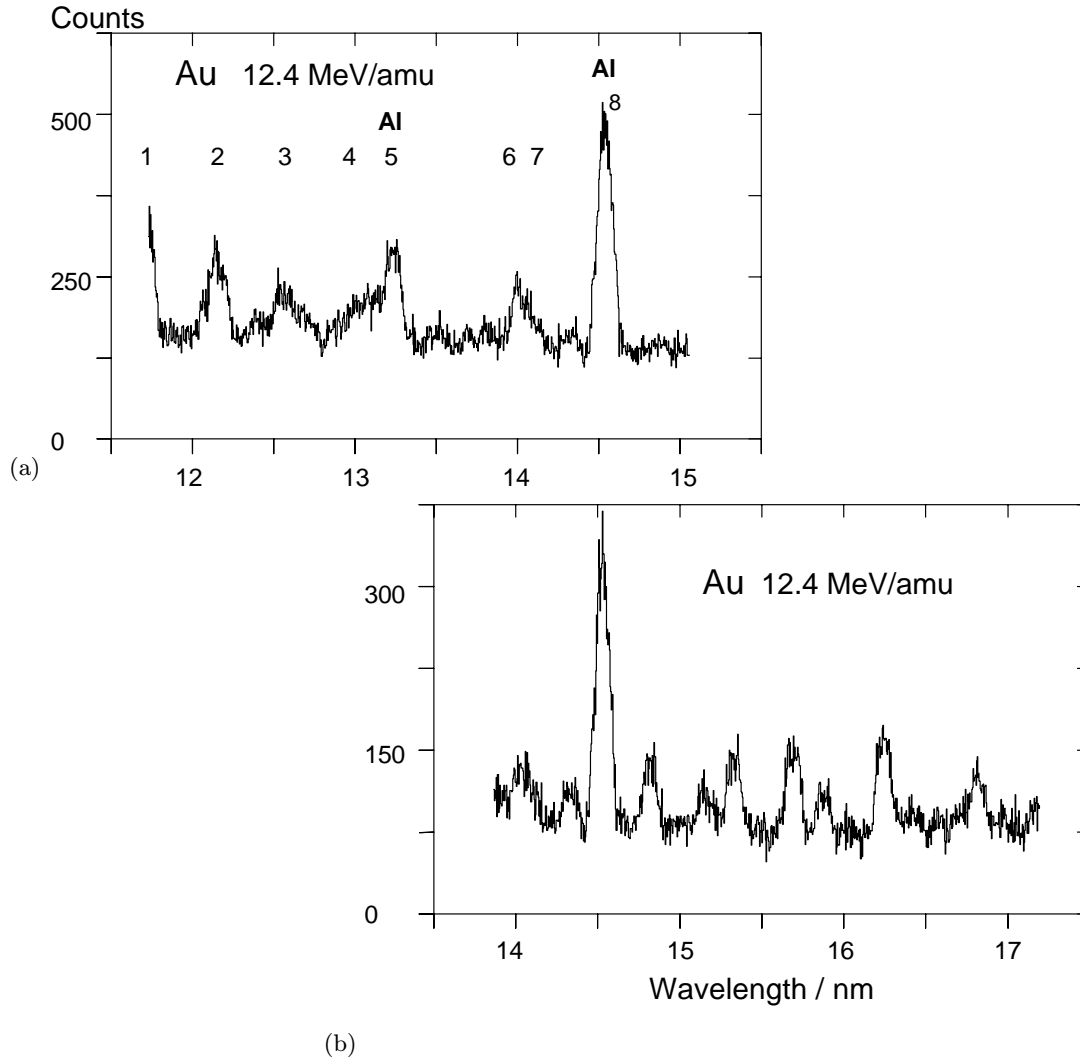


**Fig. 2.** Spectra of foil-excited Au (a) Charge-state selected ion beam ( $q = 66+$ ), foil thickness  $50 \mu\text{g}/\text{cm}^2$ , b) Charge-state selected ion beam ( $q = 67+$ ), foil thickness  $46 \mu\text{g}/\text{cm}^2$  at a specific ion energy of  $12.4 \text{ MeV}/\text{amu}$  in the vicinity of the second diffraction order image of the line of primary interest,  $3s^2 3p^2 P_{3/2}^o - 3s 3p^2 {}^4 P_{5/2}$ , in Al-like  $\text{Au}^{66+}$ . The labels refer to Table 1. Spectrum a) is the sum of 12 spectra recorded at different foil positions (delays after excitation), spectrum b) the sum of 8 delayed spectra, each of which result from about  $10^{14}$  ions.

Mg-like  $\text{Au}^{67+}$  has previously (Paper I) been reported at a wavelength of  $6.71 \pm 0.05 \text{ nm}$ . At the presently lower ion energy, we do not find any line at the above wavelength, which probably is also due to the experimental arrangement with the pick-up foil. Our delayed spectra permit coarse lifetime estimates for some other weak lines, but these are too imprecise for meaningful discussions. The only other spectral line in our spectra that is amenable to the measurement of a sufficient set of delayed spectra and thus to useful lifetime measurements, at  $6.60 \text{ nm}$ , is seen as a candidate for the transition  $3s^2 3p^2 P_{1/2}^o - 3s 3p^2 {}^4 P_{1/2}$  in the Al-like ion  $\text{Au}^{66+}$ , as already claimed in Paper I.

For the lifetime measurements, a sequence of spectra was recorded at up to 15 positions of the exciter foil. The peaks in the individual spectra were analyzed, and decay curves (Fig. 3) were constructed from the signal summed

over the line profile of a given spectral feature. The field of view of the detection system at the ion beam (about  $10 \text{ mm}$  in front of the slit jaws) was about  $250 \mu\text{m}$  wide (slit setting of  $100 \mu\text{m}$ , plus an allowance for the aperture ratio of the spectrometer). This corresponds to a time of flight of the ions of about  $5 \text{ ps}$ . This time resolution was quite sufficient for the experimental problem.

Decay curves were analyzed by multi-exponential fits, taking the spatial resolution of the detection system into account [25]. The superior ANDC formalism [26], which explicitly deals with the cascades repopulating the level under study, was not employed, because no cascade measurements were feasible (the corresponding cascade transitions are in the x-ray wavelength range and originate from levels with sub-ps lifetimes). However, with primary decays so much longer-lived than most of the cascade levels,

**Table 1.** Observed lines and identifications in the spectra of foil excited Au ions at a specific energy of 12.4 MeV/amu, in the vicinity of the second diffraction order image of the line of primary interest,  $3s^23p^2P_{3/2}^o-3s3p^2^4P_{5/2}$ , in Al-like Au<sup>66+</sup>. The elemental symbols Al and Si denote the isoelectronic sequences. All lines are assumed to appear in second diffraction order. The running index refers to Figure 1. Lifetime predictions with an asterisk (\*) have been corrected for the measured transition energies. Lifetime components (probably primary decay plus cascade) without error bars are rough results which may be useful for future guidance.

Index	Wavelength $\lambda$ (nm)		Sequence and transition	Lifetime $\tau$ (ps)	
	Observed	Reference		Observed	Reference
1	5.85			4, 50	
2	6.05			5, 31	
3	6.20				
4	6.51	6.483 [17]	Si $3s^23p^2^3P_1-3s3p^3^5S_2^o$		27.7 [17]
5	$6.60 \pm 0.02$	6.525 [11]	Al $3s^23p^2P_{1/2}^o-3s3p^2^4P_{1/2}$	$22 \pm 4$	17.8 [11] 18.4*
6	7.00	6.840 [17]	Si $3s^23p^2^3P_2-3s3p^3^5S_2^o$	$37 \pm 7$	27.7 [17]
7	7.08				
8	$7.27 \pm 0.01$	6.983 [11]	Al $3s^23p^2P_{3/2}^o-3s3p^2^4P_{5/2}$	$50.5 \pm 2$	53.2 [11] 60.0*

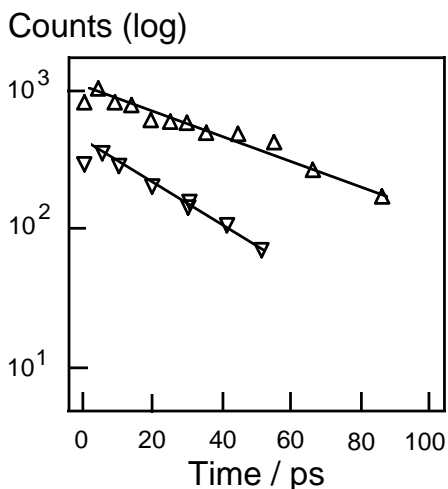


**Fig. 3.** Decay curves of lines 5 and 8 in the spectrum shown in Figure 1, which we ascribe to the transitions  $3s^23p^2P_{1/2}^o-3s3p^2^4P_{1/2}$  (lower data  $\nabla$ ) and  $3s^23p^2P_{3/2}^o-3s3p^2^4P_{5/2}$  (upper data  $\Delta$ ) in the Al-like ion Au<sup>66+</sup>. The statistical error bars of the individual data are close to the symbol size.

the chosen method is known to yield acceptable results with little systematic error (Tab. 1). The error estimates reflect the limits of the evaluation method as well as the statistical quality of the data. The lifetime analysis corroborated the identifications of two lines in the delayed spectra as the specified intercombination transitions in Al-like ions.

## 4 Comparison of experiment and theory

For the  $3s^23p^2P^o-3s3p^2^4P$  intercombination lines in Al-like ions our experiment yields the transition wavelength and first lifetime data on two fine structure levels in a range of  $Z$  far above the previous data range [7, 14]. Here the wavelengths are reasonably close to those predicted by Huang on the basis of MCDF calculations [11]. However, the 4% deviation of the transition energy for the Au<sup>66+</sup>  $3s^23p^2P_{3/2}^o-3s3p^2^4P_{5/2}$  line is larger than that observed at low  $Z$ , though not as large as a simple extrapolation of the related data trend on the Si isoelectronic sequence in [16] might suggest. Transition rates depend on the third power of the transition energy. Therefore Huang's prediction of a  $3s3p^2^4P_{5/2}$  level lifetime of 53 ps, which is based on a transition wavelength of 6.983 nm, needs to be semi-empirically adjusted to take the measured wavelength of 7.265 nm into account. This would move the prediction to about 60 ps, whereas the experiment yields  $(50.5 \pm 2)$  ps (Fig. 4). The present wavelength and lifetime results indicate that systematic errors might be present in the calculation, which may cause a fortuitous agreement with experiment at low nuclear charge. For the other observed transition of the same multiplet,  $3s^23p^2P_{1/2}^o-3s3p^2^4P_{1/2}$ , the experimental wavelength differs by only 1.5% from Huang's prediction. This implies a correction of the predicted lifetime from 17.8 ps to 18.4 ps. We find a lifetime of  $22 \pm 4$  ps. While at the low signal level encountered this is not a precise result, it is on the long side of the predicted value, contrary to the finding for the  $J = 5/2$  level. Thus we conclude that within a given multiplet of ground state transitions, the quality of wavelength and transition rate predictions may be different from line to line, or for  $j = 1/2$  and  $j = 3/2$  wavefunctions. While generally the relativistic MCDF calculations are expected to be more precise at high  $Z$  than

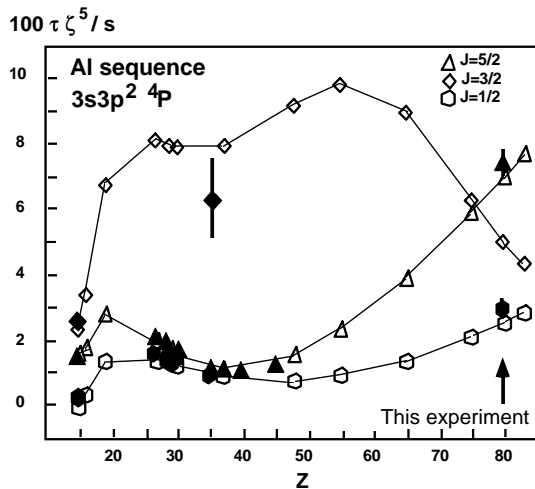


**Fig. 4.** Scaled lifetime data on the Al sequence.  $\zeta$  is the charge seen by a nominal valence electron (ion charge + 1). The theoretical lifetime data (open symbols, connected by eye-guiding lines) are from Huang [11]. However, because the proper wavelengths for most elements are not yet known, the calculated lifetime data have not been corrected for the deviations of the transition energies from measured data. This may be a small effect at low  $Z$ , but it amounts to more than 10% at the high- $Z$  end of the sequence. For example, according to our line identification for the  $J = 5/2$  level decay, the corresponding predicted lifetime for  $Z = 79$  would not be below our measured data point, but above. The experimental lifetime data (full symbols) are from [7, 9, 14, 28] and this work.

at low  $Z$ , this seems not to be the case here. More detailed calculations are definitely wanted.

The intercombination transitions  $3s^23p^2 \ ^3P_{1,2} - 3s3p^3 \ ^5S_2$  in the Si I isoelectronic sequence are well established in the first third of the isoelectronic sequence [9, 27]. They might be expected to show in our Au spectra with an intensity comparable to that of the others because of the charge state distribution, and indeed there are several lines which would come close to the pattern predicted by Huang [17]. However, apparent discrepancies in the middle of the periodic table (data on Kr, Y, Zr and Nb [16]) with trend analyses based on data for lower- $Z$  Si-like ions put severe doubt on the validity of any guidance by the available MCDF calculations for high- $Z$  ions. The present data, which are better resolved and closer in charge state distribution to Si-like ions than those of Paper I, do not confirm the tentative assignments of the  $3s^23p^2 \ ^3P_{1,2} - 3s3p^3 \ ^5S_2$  transitions presented in Paper I. The new candidate lines at 6.51 nm (part of a blend of several lines) and at 7.00 nm (partly blended) are fairly close in wavelength to Huang's prediction and have about the predicted intensity ratio of 1:1. Data for intermediate elements will be necessary to validate either theory or the sudden deviation from the calculated trend as claimed by Bengtsson *et al.* [16].

## 5 Conclusion

The present study is a step forward in the quest of testing atomic structure calculations of relatively simple many-electron systems in the high  $Z$  regime. The experimental state of the art of time-resolved EUV spectroscopy, of very energetic beams of highly charged ions, has reached a high level with good control over experimental conditions, at the considerable cost of accelerator time. Systematic studies of high quality are now feasible. For example, it is possible to “dial up” the spectra of specific ionic charge states by a suitable choice of ion energy, pre-stripper and pick-up foil, to perform observations in several diffraction orders to ascertain identifications and avoid spectral blends or to place the lines of interest near to suitable wavelength calibration lines. The recording of prompt versus delayed spectra can corroborate identifications and yields information on transition probabilities.

This demonstration study, of a high- $Z$  Al-like ion, that is in the realm of massive relativistic effects, yields the expected general confirmation of the gross predictive power of relativistic calculations for wavelengths (at the few-percent level for  $\Delta n = 0$  transitions in the lowest open shell) and radiative lifetimes (in the 20% range). The new experimental information is more precise than the theoretical prediction, and it could be used to investigate what parts of the calculation might need to be improved. The precision of some MCDF calculations applied to one- and two-electron systems, however, is much higher, and we only can speculate whether the present shortcomings of calculations for a (basically) three-electron system are a matter of computing power, or whether a judicious choice of wave functions might do better even without the highest computing power.

Experiment, even with such few-electron systems, shows several spectral lines in the range of uncertainty of the wavelength prediction. Time-resolved spectroscopy then clearly helps to discriminate among alternative line identifications. The observed error in the predicted transition probabilities only partly relates to the insufficient precision in the calculation of transition energies. As the transition probabilities depend more strongly than the transition energies on the radial part of the wave functions, better radial wave functions (or the inclusion of many more configurations) seem needed. In order to connect the new high- $Z$  data with those at low  $Z$ , it would be advantageous to obtain comparably clean data for a few elements in between, for example for I and/or Xe and a few others. This range would also be promising for a lifetime measurement of the  $J = 3/2$  level, which differs from the other levels because of a peculiarity of a matrix element.

We gratefully acknowledge the GSI crew of operators who cared to provide stable ion beams, and the help by the beam coordinator, J. Gerl. T.J.M. Zouros deserves thanks for his willingness to assist with the experiment and for interesting discussions. This study benefitted from financial support by the Deutsche Forschungsgemeinschaft, by a project GSI-Universität Giessen and by travel support from Université Liège.

## References

1. V.A. Zilitis, *Opt. Spect.* **26**, 793 (1994).
2. E. Träbert, J. Doerfert, J. Granzow, R. Büttner, U. Staude, K.-H. Schartner, P. Rymuza, P.H. Mokler, L. Engström, R. Hutton, *Phys. Lett. A* **188**, 355 (1994).
3. E. Träbert, J. Doerfert, J. Granzow, R. Büttner, U. Staude, K.-H. Schartner, P. Rymuza, L. Engström, R. Hutton, *Z. Phys. D* **32**, 295 (1995).
4. P.C. Ojha, F.P. Keenan, A. Hibbert, *J. Phys. B* **21**, L395 (1988).
5. E. Träbert, *Physica Scripta* **48**, 699 (1993).
6. R. Hutton, S. Huldt, B. Nyström, I. Martinson, K. Ando, T. Kambara, Y. Kanai, Y. Nakai, Y. Awaya, *Nucl. Instrum. Meth. B* **98**, 48 (1995).
7. R. Hutton, *Physica Scripta T* **73**, 25 (1997).
8. K.T. Cheng, W.R. Johnson, *Phys. Rev. A* **16**, 263 (1977).
9. E. Träbert, R. Hutton, I. Martinson, *Z. Physik D* **5**, 125 (1987).
10. E. Träbert, R. Hutton, I. Martinson, *Mon. Not. R. astron. Soc.* **227**, 27p (1987).
11. K.-N. Huang, *At. Data Nucl. Data Tables* **34**, 1 (1986).
12. A. Farrag, E. Luc-Koenig, J. Sinzelle, *At. Data Nucl. Data Tables* **27**, 539 (1982).
13. C. Jupén, B. Denne, I. Martinson, *Physica Scripta* **41**, 669 (1990).
14. E. Träbert, H.G. Berry, R.W. Dunford, J. Suleiman, E.W. Kanter, C. Kurtz, S. Cheng, A.E. Livingston, K.W. Kukla, F.G. Serpa, L.J. Curtis, *Phys. Rev. A* **47**, 3805 (1993).
15. C. Jupén, L.J. Curtis, *Physica Scripta* **53**, 312 (1996).
16. P. Bengtsson, K. Ando, T. Kambara, Y. Awaya, R. Hutton, *Physica Scripta T* **73**, 81 (1997).
17. K.-N. Huang, *At. Data Nucl. Data Tables* **32**, 503 (1985).
18. E. Träbert, P.H. Heckmann, R. Hutton, I. Martinson, *J. Opt. Soc. Am. B* **5**, 2173 (1988).
19. R. Büttner, B. Kraus, K.-H. Schartner, F. Folkmann, P.H. Mokler, G. Möller, *Z. Phys. D* **22**, 693 (1992).
20. R.O. Sayer, *Rev. de Phys. Appl.* **12**, 1543 (1977).
21. K. Shima, N. Kuno, M. Yamanouchi, H. Tawara, *At. Data Nucl. Data Tables* **51**, 173 (1992).
22. B. Kraus, GSI-Report 91-16 (GSI Darmstadt 1991); B. Kraus, K.-H. Schartner, F. Folkmann, A.E. Livingston, P.H. Mokler, *Proc. SPIE* **1159**, 217 (1989).
23. P.H. Mokler, Th. Stöhlker, R. Büttner, K.H. Schartner, *Nucl. Instrum. Meth. B* **83**, 37 (1993).
24. Y.-K. Kim (private communication).
25. E. Träbert, H. Winter, P.H. Heckmann, H.v. Buttler, *Nucl. Instrum. Meth.* **135**, 353 (1976).
26. L.J. Curtis, H.G. Berry, J. Bromander, *Phys. Lett. A* **34**, 169 (1971).
27. C. Jupén, I. Martinson, B. Denne-Hinnov, *Physica Scripta* **44**, 562 (1991).
28. A.G. Calamai, P.L. Smith, S.D. Bergeson, *Astroph. J.* **415**, L59 (1993).